ACS Sustainable Chemistry & Engineering

pubs.acs.org/journal/ascecg



Research Article

# Time-Resolved Analysis of Lignocellulose Extraction in a Biphasic, Acid-Catalyzed Flow-through System

Leonie Schoofs,[⊥] Henry Hilker,[⊥] Niclas Conen, Andreas Jupke, Holger Klose,* and Philipp M. Grande*

Cite This: *ACS Sustainable Chem. Eng.* 2026, 14, 7099−7108

Read Online

ACCESS | Metrics & More | Article Recommendations | Supporting Information

**ABSTRACT:** Kinetic studies of lignocellulose fractionation clarify mechanisms of biomass deconstruction but are challenged by substrate heterogeneity. Here, flow-through biphasic OrganoCat (OrganoCatFT) was used to fractionate beech wood and Miscanthus at 140 °C, 160 °C and 180 °C with 5 min sampling. Monosaccharide time courses showed rapid hemicellulose breakdown: xylose dominated the aqueous phase yet remained incompletely extracted, peaking at approximately 10 min at 160 °C−180 °C and at 20−25 min at 140 °C. At 140 °C, galacturonic acid was unexpectedly abundant (approximately 26% of extracted sugars from beech; approximately 10% from Miscanthus), indicating enhanced pectin accessibility under OrganoCatFT. Glucose yields increased with temperature and exceeded native glucan contents in hemicelluloses, consistent with contributions from starch, hemicellulosic glucan and limited cellulose hydrolysis. Kinetic fitting for beech required fast and slow xylan fractions with Arrhenius activation energies of 105 kJ mol$^{-1}$ (fast) and 144 kJ mol$^{-1}$ (slow) and an increasing fast fraction, $\varphi$ = 0.208−0.634 (140 °C−180 °C). Miscanthus yielded higher xylose at 160 °C (106 mg g$^{-1}$ vs 37 mg g$^{-1}$ at 140 °C) but lower at 180 °C (80 mg g$^{-1}$) due to furfural formation; glucose stayed ≤2.4 mg g$^{-1}$. Thus, biomass-specific xylan architecture governs early hydrolysis, whereas cellulose conversion is only weakly temperature dependent in this range.

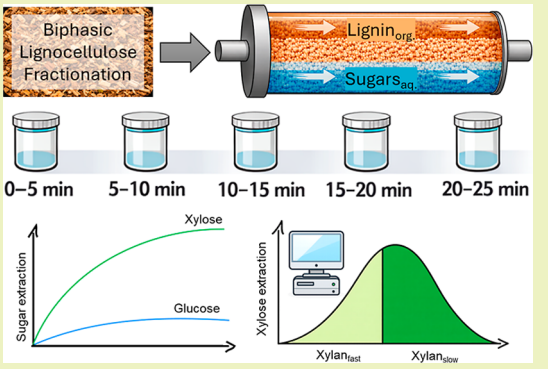


**KEYWORDS:** *biorefinery, lignocellulose, kinetic, flow-through, organocat*



## INTRODUCTION

To design effective pretreatment strategies and maximize biomass valorization, it is important to understand how lignocellulosic biomass responds to chemical processing. Plant cell walls form a multipolymer composite of cellulose, hemicelluloses and lignin whose constituents can be selectively solubilized depending on process conditions.[1] Tracking these solubilized fractions over time provides a means to resolve the sequence of extraction and to relate observed release patterns to biomass composition and structural features.

Acid-based pretreatments are employed in lignocellulosic biorefineries due to their ability to selectively hydrolyze hemicellulose and enhance lignin solubility and cellulose accessibility.[2] These processes disrupt the hemicellulose−lignin matrix and can facilitate the depolymerization of lignin through cleavage of $\beta$-*O*-4 linkages.[1,3,4] However, the effectiveness of such treatments depends heavily on fine-tuning process conditions to limit the formation of degradation products such as furfural and 5-hydroxymethylfurfural, which can inhibit downstream (bio)catalytic conversion.[1] Understanding acid-catalyzed reactive extraction is therefore essential for optimizing pretreatment severity and adapting strategies to biomass-specific and product-oriented requirements.[5−7]

The recalcitrance of lignocellulosic biomass is closely linked to the structural organization of its major components-cellulose, hemicellulose, and lignin. In particular, the physical proximity and chemical linkages between lignin and hemicellulose can hinder access to carbohydrate domains, thereby limiting saccharification yields and overall process efficiency.[1] It is important to note that extractability is not uniform. This is due to interspecies differences, as well as spatial variation within tissues, resulting in domains that respond differently to pretreatment.[5] The sequential deposition of cell wall polymers, initially cellulose and hemicellulose, followed by lignin, leads to a dense, interpenetrating matrix in which lignin encapsulates and protects polysaccharides, thereby reinforcing these differences in accessibility.[8] Recent insights into xylan conformation further underscore this structure-process relationship, for example, xylan binding to cellulose in a 2-fold helical arrangement contributes to wall rigidity and enzymatic resistance.[9] Mild pretreatment approaches that selectively disrupt lignin structure while preserving carbohydrate integrity have therefore emerged as promising avenues for improving

Received: June 6, 2025
Revised: March 20, 2026
Accepted: March 23, 2026
Published: April 6, 2026

biomass fractionation efficiency.[1] Ultimately, advancing biorefinery processes requires an interdisciplinary approach that integrates structural biology, polymer chemistry, and process engineering to effectively deconstruct lignocellulosic biomass.[1,5]

This study focuses on the time-resolved analysis of an acidic, biphasic flow-through process,[10] leveraging these advancements to explore the kinetics and apparent accessibility-limited behavior of biomass deconstruction. To this end, time-resolved sampling under continuous flow-through OrganoCat conditions is combined with a kinetic model that distinguishes between fast and slow xylan domains. In contrast to batch pretreatment, continuous removal of solubilized products facilitates the estimation of apparent domain-specific hydrolysis kinetics from early time data and provides quantitative descriptors (e.g., $\varphi$) that reflect temperature-dependent accessibility rather than only overall yields. These insights support a more quantitative understanding of fractionation dynamics and inform process optimization for industrial biomass processing.

## MATERIALS AND METHODS

Oxalic acid and 2-methyltetrahydrofuran were sourced from suppliers Carl Roth and Sigma-Aldrich (Germany) and utilized without additional purification. Beech wood and Miscanthus biomass were predried, and underwent milling using a cutting mill (SM 200, Retsch, Haan, Germany) fitted with a 1 mm sieve.

### Compositional Analysis of Lignocellulose

Was conducted adhering to established procedures with slight modifications for wet chemistry analysis of lignocellulose,[11] the following steps were undertaken: Initially, alcohol-soluble components were extracted, and subsequent analyses focused solely on the alcohol-insoluble residues (AIR). All samples underwent enzymatic breakdown of starch to produce destarched lignocellulose samples (dAIR). Lignin content was determined using the acetyl bromide soluble lignin (ABSL) method, while crystalline cellulose levels were quantified using the Updegraff technique, as outlined by Foster et al.[12,13] The analysis of noncellulosic polysaccharide composition within dAIR involved hydrolysis with trifluoroacetic acid (TFA) followed by detection using high-performance anion-exchange chromatography with pulsed amperometric detection (HPAEC-PAD), following the methodology described by Damm et al.[11] Total acetate content was assessed using the acetic acid kit (KACE-TRM, Megazyme, Wicklow, Ireland).

### Processing of Lignocellulose

Was conducted as described before, using a flow-through reactor system for biomass fractionation.[10] The setup included a stainless-steel tube with dimensions of 4.6 mm inner diameter and 15 cm length as the reactor, positioned within an aluminum heating block on a heating plate. Temperature regulation was achieved using a thermometer connected to the heating plate. Stainless-steel frits with a pore size of 2 $\mu$m were installed at both ends of the reactor to contain particles.

A 0.1 M aqueous oxalic acid solution and 2-methyltetrahydrofuran (2 MTHF) were supplied from solvent bottles and delivered simultaneously using a high-pressure dosing pump (C09-20.2-200 DK-VA, Fink Chem + Tec GmbH) equipped with two individually controlled pulp heads, capable of up to 200 bar pressure. The solvents were conveyed through 1/16″ stainless steel tubing with a flow rate of 0.2 mL min$^{-1}$ and mixed at a T-valve, which connected to the reactor. After passing through the reactor, the solvents exited via a 1/16″ stainless steel capillary, immersed in an ice bath to cool rapidly. A backpressure valve maintained a constant reactor pressure of 70 bar, minimizing solvent loss.

Approximately 800 mg of beech wood or Miscanthus was loaded into the reactor under light pressure, and the setup was vertically oriented. Solvent flow commenced until steady exit was observed, after which the reactor was sealed and pressurized to 70 bar. Following leak check, the reactor was inserted into the preheated heating block, and solvent pumping began immediately at equal rates. Upon completion of the desired processing time, pumps were halted, and the reactor cooled in an ice bath.

The solid pulp was removed, washed with 3 × 30 mL of water using a filter, and liquid phases were separated via pipet. Oxalic acid was precipitated from the organic phase using an equal volume of 0.2 M $CaCl_2$, while the organic phase was concentrated using a rotary evaporator and vacuum-dried for 24 h. Lignin yields were determined gravimetrically, and sugar concentrations and compositions in the aqueous phase were analyzed using high-performance anion-exchange chromatography with pulsed amperometric detection (HPAEC-PAD). A detailed description of the setup is provided in Schoofs et al. 2024.[10]

### Quantitative Kinetic Analysis

Of sugar species in the pretreatment was conducted based on irreversible and pseudo first order reactions. The analysis was limited to glucose and xylose as the most relevant sugars by fraction. Xylan was distinguished into slow (s) and fast (f) reacting fractions for the hydrolysis to xylose reflecting their differing reactivities.[14,15] The respective fraction was defined as

$$\varphi(T) = \frac{w_f(T)}{w_{ges}} \tag{1}$$

Instead of being a fixed structural property of the biomass, $\varphi(T)$ is interpreted as an effective accessible xylan fraction that increases with temperature due to thermally induced swelling and progressive disruption of lignin-xylan interactions,[14] which exposes initially protected xylan domains to hydrolysis. Formally, the slow and fast reacting fraction converts independently into soluble sugars. In addition, degradation of dissolved xylose to furfural and lumped secondary degradation products was included as an irreversible pseudo-first-order side reaction. For modeling, cellulose and xyloglucan were lumped into a single structural carbohydrate fraction to simulate glucose formation, while starch was treated as a separate fraction. This lumping was necessary because (i) these glucose sources cannot be distinguished analytically in the hydrolysate, (ii) the low glucose yields preclude robust estimation of separate rate constants, and (iii) hydrolysis of starch is known to be faster than for xyloglucan and cellulose. The chosen strategy enables parameter identifiability and robust estimation from the available experimental data set.[16,17] The fitted parameters should therefore be interpreted as effective phenomenological constants reflecting aggregate hydrolysis behavior rather than intrinsic polymer properties. Degradation of glucose was not considered, as no formation of 5-hydroxymethylfurfural (HMF) or other glucose-derived degradation products could be detected in the liquid hydrolysates within analytical uncertainty. The overall modeled reaction network can thus be formulated as depicted in Scheme 1.

Temperature dependency of the rate constants $k_i$ was modeled using a modified form of the Arrhenius equation to reduce the correlation between pre-exponential factor $k_{i,ref}$ and activation energy $E_{i,A}$[18]

$$k_i = k_{i,ref}\exp\left(\frac{-E_{i,A}}{R}\left(\frac{1}{T} - \frac{1}{T_{ref}}\right)\right) \tag{2}$$

The reference temperature $T_{ref}$ was set to 160 °C. Water was assumed to be abundant and constant, so it was excluded from the calculation of the reaction rates. Reaction kinetics of xylose degradation were taken from literature since furfural was not quantified in the present study.[19,20]

The flow-through reactor was represented as a one-dimensional series of 50 ideal continuous stirred-tank reactors (CSTR-cascade) of equal segment volume, which approximates transient plug-flow behavior by suppressing axial back-mixing while retaining robust numerics. The number of 50 CSTR was selected because it exhibits


https://doi.org/10.1021/acssuschemeng.5c05534
ACS Sustainable Chem. Eng. 2026, 14, 7099−7108

**Scheme 1. Considered Reactions for the Hydrolysis of Beech and Miscanthus**

$$\text{Xylan}_s + n\ \text{H}_2\text{O} \xrightarrow{k_{sx}} n\ \text{Xylose}$$

$$\text{Xylan}_f + n\ \text{H}_2\text{O} \xrightarrow{k_{fx}} n\ \text{Xylose}$$

$$\text{Xylose} \xrightarrow{k_{degx}} \text{Furfural} + 3\text{H}_2\text{O}$$

$$\text{Cellulose} + n\ \text{H}_2\text{O} \xrightarrow{k_{sg}} n\ \text{Glucose}$$

$$\text{Xyloglucan} + n\ \text{H}_2\text{O} \xrightarrow{k_{sg}} n\ \text{Glucose}$$

$$\text{Starch} + n\ \text{H}_2\text{O} \xrightarrow{k_{fg}} n\ \text{Glucose}$$

numerical convergence while maintaining computational efficiency. An exemplary convergence plot of beech hydrolysis at 140 °C is shown in the Supporting Information in Figure S1.

The solid lignocellulose feed was modeled as a stationary packed bed uniformly distributed across segments.

For each dissolved species $j$ in segment $k$, the unsteady CSTR balance reads

$$\frac{dc_{j,k}}{dt} = \frac{1}{\tau_k}(c_{j,k-1} - c_{j,k}) + \sum_i k_{j,i} c_{j,k} \tag{3}$$

where $\tau_k$ is the residence time of a segment $k$ and $k_{j,i}$ the kinetic constant of component $j$ of reaction $i$. The reaction was assumed to be isochoric and external film resistances at the solid−liquid interface were assumed nonlimiting due to high specific surface of milled biomass and continuous flushing, while intraparticle diffusion was incorporated implicitly into effective kinetic constants. The residence time was assumed constant for each segment over the reaction time and was calculated using the densities of the cell walls (without pore volumes) of respective biomass

$$\tau_k = \frac{\epsilon V_k}{Q} = \left(1 - \frac{m_{\text{Bio}}/\rho_{\text{Bio}}}{V_k}\right) \times \frac{V_k}{Q} \tag{4}$$

where $V_k$ is the porosity of a segment, $Q$ the mass flow, $m_{\text{Bio}}$ the initial biomass mass and $\rho_{\text{Bio}}$ the respective biomass cell wall density. These are 1520 kg/m$^3$ for beech and 940 kg/m$^3$ for Miscanthus.[21,22]

Modeled liquid species were assumed to be not soluble in the 2 MTHF phase.

The resulting ordinary differential equation system from the N-tank cascade was integrated in Python with explicit adaptive-step Runge−Kutta integrator of order 4(5) (RK45). N was increased until concentration profiles converged, ensuring proximity to the plug-flow limit for the operating conditions. Parameters were estimated by minimizing the squared deviation between simulated outlet segment totals using a nonlinear least-squares algorithm with a trust-region framework.

### 2D-$^1$H−$^3$C-HSQC-NMR

Analysis was employed to investigate lignin. For each sample, 25 mg of lignin was dissolved in 0.75 mL of deuterated dimethyl sulfoxide (DMSO-$d_6$) after stirring at 60 °C for 2 h until complete dissolution of the biomass. The measurements were conducted on a Bruker AVANCE 600 MHz NMR spectrometer using the standard pulse sequence "hsqcetgpsisp.2". Spectral parameters included a spectral width of 16 ppm in the F2 (1H) dimension with 2048 data points (TD1) and 240 ppm in the F1 (13C) dimension with 256 data points (TD2). Each spectrum was acquired with 128 scans (SN), an interscan delay (D1) of 1 s, and an acquisition time of 10 h. Chemical shifts were referenced to the DMSO signal ($\delta$(1H) = 2.500 ppm; $\delta$(13C) = 39.52 ppm).

The signals corresponding to monomer units and linkages were integrated and compared with established lignocellulose structures from literature ref 23 The sum of aromatic units (Σ(arom.)) was calculated using the formula

$$\Sigma(\text{arom.}) = (S_{2,6}/2) + G_2 + (H_{2,6}/2)$$

the percentage of each unit was calculated as

$$S = (S_{2,6}/2)/\Sigma(\text{arom.}) \times 100\%$$

$$G = G_2/\Sigma(\text{arom.}) \times 100\%$$

$$H = (H_{2,6}/2)/\Sigma(\text{arom.}) \times 100\%$$

Linkages are expressed as per 100 monomer units. To account for overlapping peaks, $\beta$-$O$-4 linkages are determined exclusively from the $\alpha$ proton signal. $\beta-\beta$ and $\beta$-5 linkages utilize all signals associated with their respective linkage types. Calculation of linkages followed these specific formulas: The linkages were quantified using the following formulas

$$\beta\text{-}O\text{-}4\text{linkages} = \alpha\beta - O - 4/\Sigma(\text{arom.}) \times 100\%$$

$$\beta-\beta\text{linkages} = (\alpha\beta - \beta + \beta\beta - \beta + \gamma\beta - \beta)/\Sigma(\text{arom.}) \times 100\%$$

$$\beta\text{-}5\text{linkages} = (\alpha\beta - 5 + \beta\beta - 5 + \gamma\beta - 5)/\Sigma(\text{arom.}) \times 100\%$$

## RESULTS AND DISCUSSION

As a typical acidic lignocellulose pretreatment, the biphasic OrganoCat technology has been previously adapted into a flow-through (OrganoCatFT) reactor.[10] In this study, the hydrolysis and extraction kinetics of acid-catalyzed lignocellulose fractionation were qualitatively assessed to elucidate structural features of the polysaccharide matrix in representative biomasses such as hardwood and grass. The biphasic flow-through system facilitated direct collection of the liquid phases postextraction, thereby minimizing precipitation effects that typically occur during reactor cooling. As described in our earlier work, the setup utilizes a heated tubular reactor where a mixture of oxalic acid and 2-methyltetrahydrofuran (2-MTHF) is continuously pumped through beech wood biomass.[10]

Due to their less ordered structures, most hemicelluloses and starch are easier to hydrolyze than cellulose. During OrganoCatFT processing, significant quantities of the hemicelluloses are disintegrated and the resulting monosaccharides are dissolved in the aqueous phase. Nevertheless, hemicellulose structure and composition vary and therefore different configurations and interactions with other cell wall constituents pose a different recalcitrance toward hydrolysis. Two distinctly different lignocellulosic materials, beech (hardwood) and Miscanthus (grass) were investigated. The resulting time-resolved analysis of polysaccharide hydrolysis in the aqueous phase provides insights into hemicellulose accessibility and the hydrolysis mechanisms during OrganoCatFT processing (Figure 1).

At elevated temperatures (160 °C−180 °C), replicate-to-replicate variability is observed to increase, most notably for Miscanthus cumulative sugar yields. Consequently, interpretations under these conditions are restricted to robust trends (e.g., early time release and degradation signatures), and replicate-level data are provided in the Supporting Information.



https://doi.org/10.1021/acssuschemeng.5c05534
ACS Sustainable Chem. Eng. 2026, 14, 7099−7108

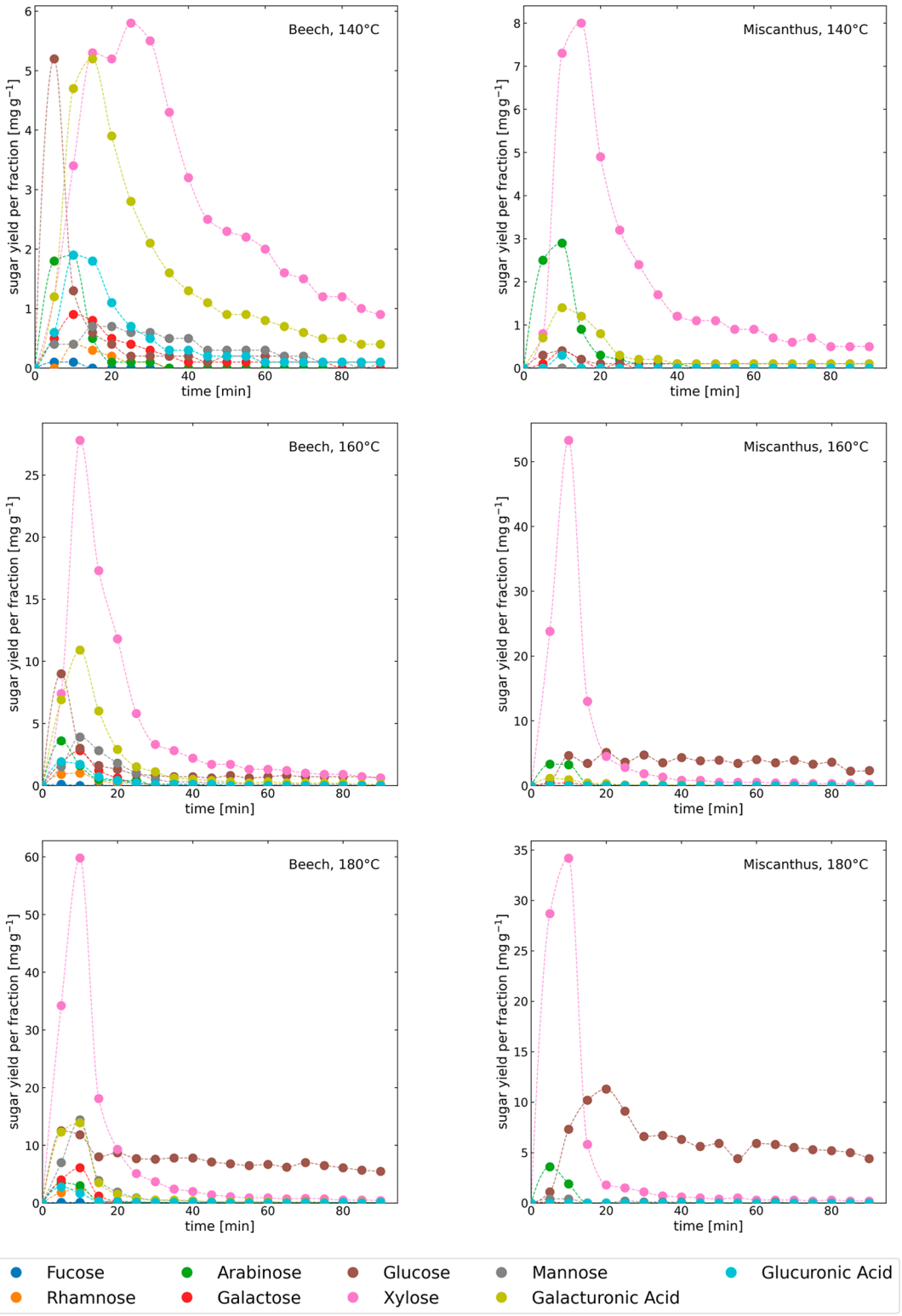


**Figure 1.** Monosaccharide yields in the aqueous phase of collected samples during OrganoCatFT processing of beech wood and Miscanthus biomass at 140 °C, 160 °C, and 180 °C. Samples were collected in 5 min intervals.

In beech wood and Miscanthus, xylose is the primary sugar in the hemicelluloses of unprocessed biomasses and in the aqueous extract (see Table S2), reflecting the high Glucuronoxylan (GX) content in the hemicelluloses. However, xylose extraction was incomplete (see Tables S1 and S2), likely due to heterogeneities in the reactor design or structural resistance from cellulose-bound GX.[9] Despite their similar xylose content, the xylan structures differ significantly from beech. Miscanthus, typical for grasses, primarily contains glucuronoarabinoxylan (GAX). These structural differences seem to result in greater accessibility and therefore higher xylose extraction yield from Miscanthus. Nevertheless, the xylose extraction in both plants still follows a similar trend: rapid release within the first 10 min, followed by a sharp



https://doi.org/10.1021/acssuschemeng.5c05534
ACS Sustainable Chem. Eng. 2026, 14, 7099−7108

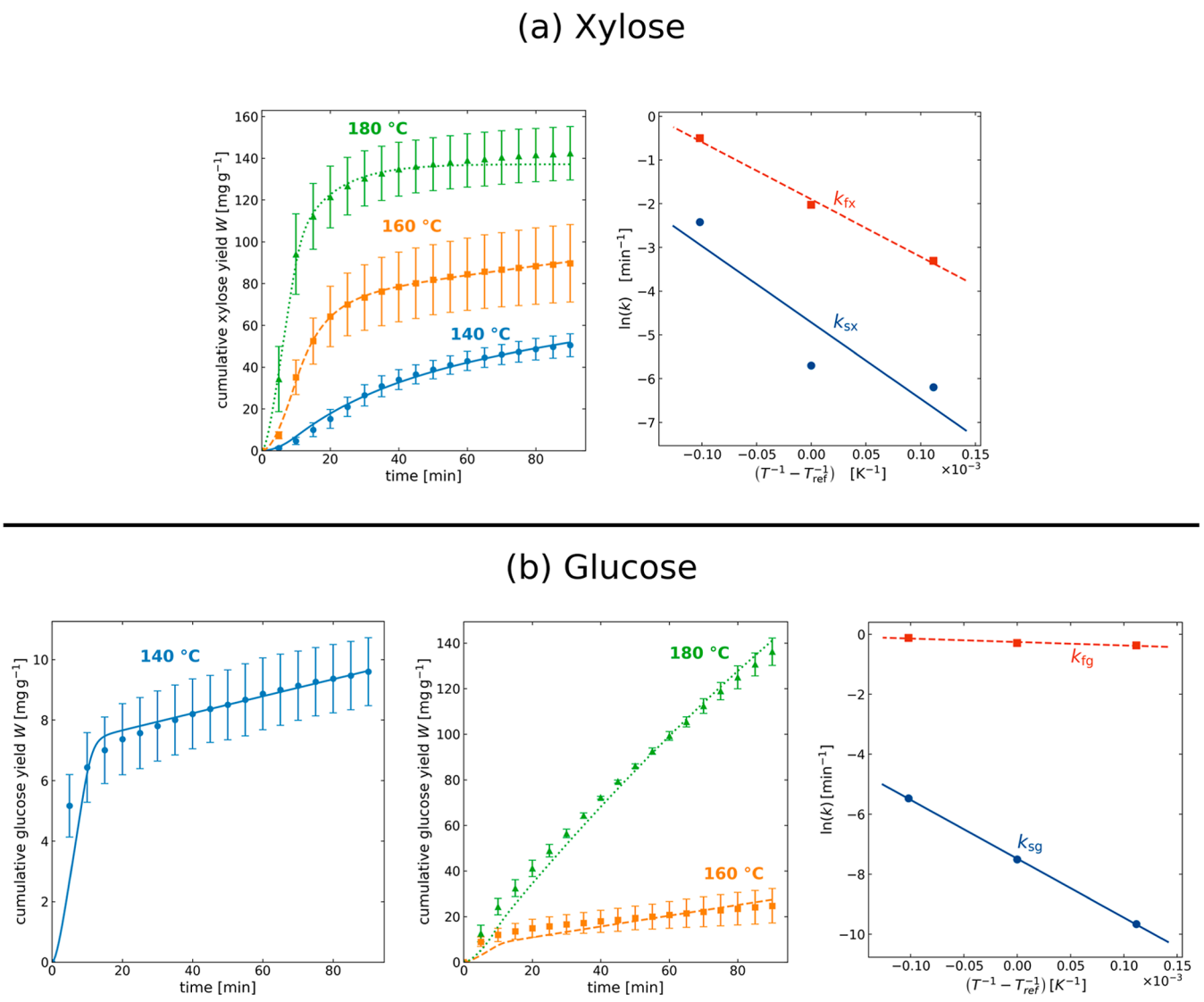


**Figure 2.** Data points represent the average cumulative sugar concentration in the aqueous hydrolysate during OrganoCatFT of beech wood biomass at 140 °C, 160 °C, and 180 °C. Samples were collected in 5 min intervals. The lines represent the model fitted from this experimental data. The right panel shows the resulting Arrhenius diagram. (a) Xylose (b) glucose.

decline. At 160 and 180 °C the Xylose extraction peaks within the first 10 min in both biomasses. At 140 °C, the extraction process peaks at 20−25 min. The delayed onset may be attributed to GX side groups and acetylation impeding hydrolysis, since acetate removal has been shown to correlate with sugar release in acid pretreatment studies.[24]

Galacturonic acid accounts for a significant fraction of sugars at 140 °C (beech wood ∼26%, Miscanthus ∼10% of total sugars extracted), exceeding its expected contribution from unprocessed beech (see Table S2). This finding is indicative of galacturonic acid groups, which are only accessible through the utilization of a complex extraction system such as Organo-CatFT, as opposed to isolated hydrolysis with an acid, a method employed for compositional analysis of untreated biomass. In Miscanthus, the signal is consistent with pectin-associated domains.[25] While the proportion of beech wood extracts varies at higher temperatures, the extraction process remains consistent across temperatures, suggesting pectin as the primary source. In Miscanthus, the process of galacturonic acid extraction exhibits an increase in efficiency with rising temperatures.

Overall glucose yield increases with temperature (see Tables S1 and S2) with starch, glucomannans, and cellulose hydrolysis contributing. Unlike other sugars, glucose extraction from beech wood follows a linear, temperature-dependent pattern after a brief, sharp peak within the first 5 min. In the case of Miscanthus, a less pronounced yet still perceptible peak is observed at 10 min, followed by the same linear pattern. This observation indicates that hydrolysis is the rate-limiting step for glucose extraction, rather than differences in accessibility.

Minor monosaccharides reflect hemicelluloses and pectin substituents to a greater extent than the main backbone cleavage. Side-group sugars (arabinose, galactose) and uronic acids (glucuronic acid) show early time maxima that are consistent with rapid cleavage of accessible substituents. Pectin-associated sugars (rhamnose, galacturonic acid) are most prominent at lower severity. Biomass-specific differences are consistent with composition. The presence of gluco-mannan-derived mannose is more pronounced in beechwood samples, while arabinose is comparatively higher in arabionox-ylan-rich Miscanthus samples. A full sugar-by-sugar breakdown is provided in the Supporting Information (Tables S1 and S2).



https://doi.org/10.1021/acssuschemeng.5c05534
ACS Sustainable Chem. Eng. 2026, 14, 7099−7108

Overall, Figure 1 highlights a rapid early hemicellulose solubilization process (xylose), a distinct low-severity pectin-associated contribution (galacturonic acid) and a temperature-driven increase in glucose release. To further investigate the most prominently extracted sugars, xylose and glucose, the experimental data were fitted with kinetic models. The mean cumulative yields of xylose and glucose extracted from beech wood over time are displayed in Figure 2.

The corresponding determined model parameters are listed in Tables 1 and 2.

**Table 1. Arrhenius Parameters of Xylan and Glucan Hydrolysis for Beech Wood**

| Product | Rate constant | $k_{i,\mathrm{ref}}$ [$\mathrm{min}^{-1}$] | $E_{i,\mathrm{A}}$ [kJ $\mathrm{mol}^{-1}$] |
|---|---|---|---|
| xylose | $k_{\mathrm{fx}}$ | $1.433 \times 10^{-1}$ | 104.81 |
| | $k_{\mathrm{sx}}$ | $8.8225 \times 10^{-3}$ | 143.76 |
| glucose | $k_{\mathrm{fg}}$ | $7.7030 \times 10^{-1}$ | 9.57 |
| | $k_{\mathrm{sg}}$ | $5.6117 \times 10^{-4}$ | 163.21 |

**Table 2. Determined Fractions of Fast Hydrolyzing Xylan for all Temperatures for Beech Wood**

| temperature | 140 °C | 160 °C | 180 °C |
|---|---|---|---|
| $\varphi$ | 0.208 | 0.461 | 0.634 |

The kinetic model for Xylan hydrolysis is based on the assumption that GX side groups and acetylation, as well as its configuration, may influence its hydrolysis. GX can exist in either a 3-fold helical screw conformation or a flattened 2-fold helical screw ribbon, which adheres to cellulose microfibrils.[9] Hardwoods typically exhibit a higher proportion of 2-fold GX compared to the 3-fold configuration.[26] GX bound to cellulose microfibrils may be more resistant to hydrolysis and consequently partially remain in the pulp.

The overall lignocellulose architecture of grasses and hardwoods shows distinct differences. GAX as predominant hemicellulose in grasses has been described to be mainly in a 3-fold screw conformation due to its dense arabinosyl substitutions.[27] This conformation preferentially binds lignin structures but has also been shown to interact with amorphous parts of cellulose in grasses.[27] The 2-fold or flat ribbon conformation binding the surface of the cellulose microfibrils is much less abundant in grasses than in hardwoods.[26,28]

The 3-fold conformation has been described as better accessible toward hydrolysis than the flat ribbon 2-fold form[29] the latter more dominant in hardwood GX. In addition, the interaction between lignin and xylan is increased in hardwood due to *S*-rich lignin, thus further reducing extractability which is supported by the amount of residual lignin and xylan in the pulp of beechwood (see Table S2). By contrast, the less polar lignin in Miscanthus, with fewer *S*-units and weaker interactions with xylan, results in a less ordered structure, facilitating faster and greater overall extraction of lignin and hemicellulose.[26,30] These structural and compositional variations underscore the differing recalcitrance and extraction efficiency of Miscanthus and beech lignocellulose.

Consequently, two distinct reaction rates for hydrolysis were incorporated into the kinetic model: $k_{\mathrm{sx}}$, representing slow xylan hydrolysis, and $k_{\mathrm{fx}}$, representing fast xylan hydrolysis. The share of fast-hydrolyzing xylan depends on the temperature.[14] Accordingly, the ratio of fast hydrolyzing to total xylan ($\varphi$) was considered as the third model parameter. As illustrated in Figure 1a, elevated temperatures enhance the xylose yield, a phenomenon that is reflected in the consistent increase in all of the model's parameters. The initial 15 min of the experiment are characterized by the predominance of easily accessible amorphous xylan. Following this initial breakdown, the curve flattens, indicating a reduction in the rate of xylan degradation due to accessing the less accessible xylan. This phenomenon is further substantiated by the activation energies $E_{\mathrm{A,sx}}$ = 144 kJ $\mathrm{mol}^{-1}$ > $E_{\mathrm{A,fx}}$ = 105 kJ $\mathrm{mol}^{-1}$. In other studies, numerous models have been implemented for different acids and biomasses, yielding activation energies ranging from 80 kJ $\mathrm{mol}^{-1}$ to 200 kJ $\mathrm{mol}^{-1}$ for diluted acids.[31] Maloney et al. for instance found in dilute acid hydrolysis of paper birch $E_{\mathrm{A,sx}}$ = 156.5 kJ $\mathrm{mol}^{-1}$; $E_{\mathrm{A,fx}}$ = 128.1 kJ $\mathrm{mol}^{-1}$, which is in the same order of magnitude as we found for beech wood.[32]

The temperature-dependent increase in $\varphi$ ($\varphi_{140\ ^\circ\mathrm{C}} < \varphi_{160\ ^\circ\mathrm{C}} < \varphi_{180\ ^\circ\mathrm{C}}$) reflects enhanced xylan accessibility through thermal swelling and disruption of lignin-xylan interactions, rather than distinct structural xylan populations. Thus, temperature-dependent increase $\varphi$ represents an effective accessible fraction that is process-dependent rather than a fixed biomass property.

Modeling glucose yield is more complex than xylose, given the greater number of sources available. Glucose can be derived from starch, glucan in hemicelluloses and glucan in cellulose.

In order to address the primary effects, the kinetic model for glucose has been simplified to a binary model to prevent overfitting. The model includes structural glucose (sg) originating from the secondary cell wall (cellulose and hemicelluloses) and glucose originating from starch (fg).

As is the case in the context of xylan hydrolysis, an increase in temperature also results in an increase in glucose yield and the associated fitting parameters. In contrast to the observable degradation of xylose, no such degradation of glucose was detected under the conditions of this study. This finding aligns with the results of a previous investigation into the batch process.[33] The initial minutes of the experiment are characterized by starch decomposition. This initial phase is followed by a state of sustained cellulose degradation.

At the onset of the reaction for all temperatures, the model deviates from the measured values. These measured values demonstrate a steepness that cannot be replicated with the available model. One possible explanation is that hemicellulose and cellulose also contain small fractions that undergo faster hydrolysis at higher temperatures. A more sophisticated model is necessary to account for these effects requiring more detailed data of this hydrolysis state, which is not possible with the current scale of the reactor. The separation of glucose released from starch and hemicelluloses poses a considerable challenge due to the low concentrations of these compounds and the complexity of their structure.

For the comparison of activation energies with literature, a limited number of values have been documented for diluted acid hydrolysis, and no data has been recorded for beech wood or Miscanthus, which were investigated in this study. For sugar cane bagasse, the activation energy ($E_{\mathrm{A}}$) for cellulose hydrolysis with sulfuric acid is approximately 175 kJ $\mathrm{mol}^{-1}$.[34]

The experimental results for the two primary sugars in Miscanthus, xylose and glucose, were simulated using kinetic models analogous to beech wood. As illustrated in Figure 3, the mean cumulative yield of xylose and glucose extracted from Miscanthus is presented as a function of time.



https://doi.org/10.1021/acssuschemeng.5c05534
ACS Sustainable Chem. Eng. 2026, 14, 7099−7108

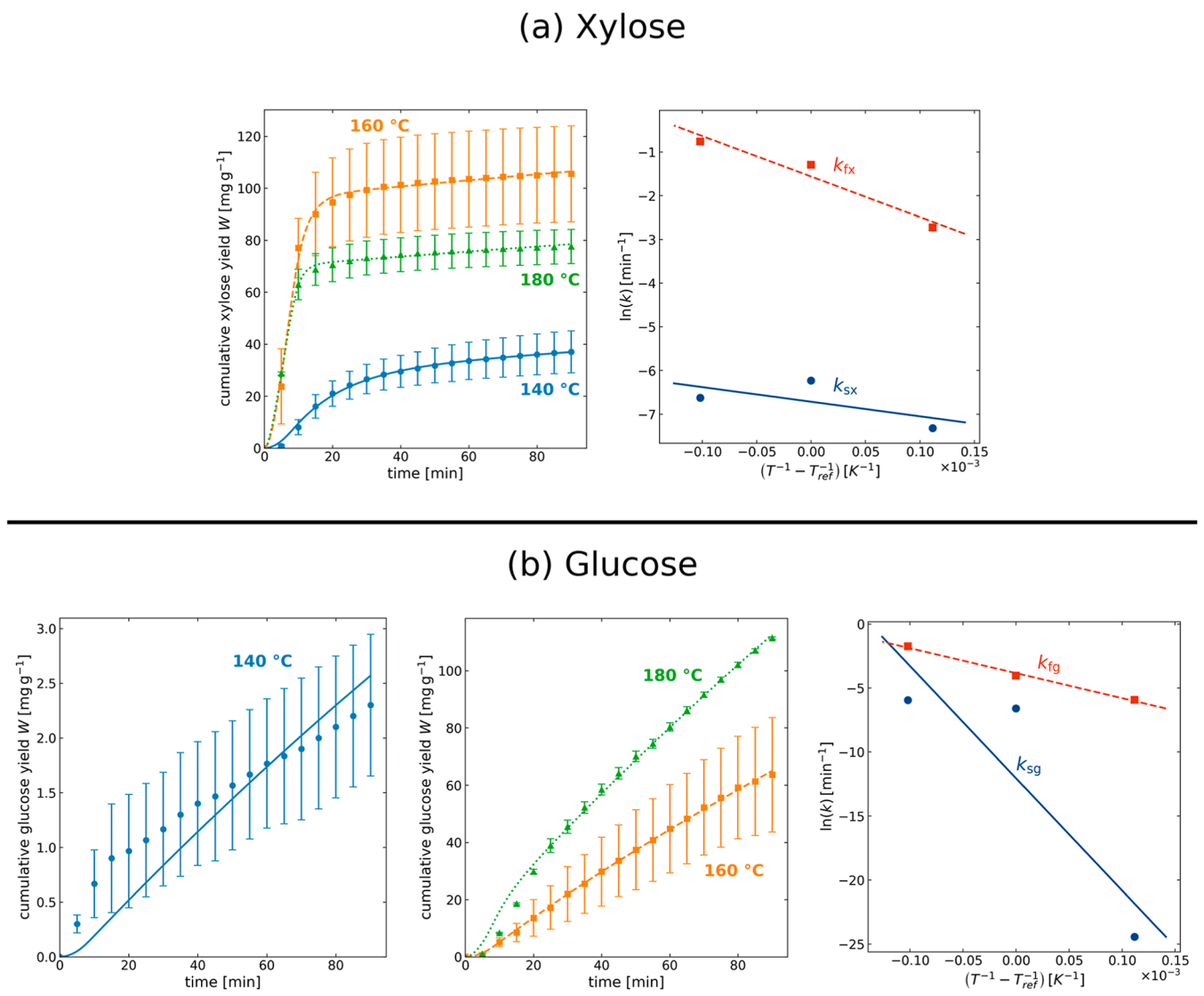


**Figure 3.** Data points represent the average cumulative sugar concentration in the aqueous hydrolysate during OrganoCatFT of Miscanthus biomass at 140 °C, 160 °C, and 180 °C. Samples were collected in 5 min intervals. The lines represent the model fitted from this experimental data. The right panel shows the resulting Arrhenius diagram. Due to the high variability in the experimental data, the Arrhenius plots shown here only have limited mechanistic meaning. (a) Xylose (b) glucose.

The corresponding determined model parameters are listed in Tables 3 and 4.

The overall xylose yield from Miscanthus increased from 140 °C (37 mg $g^{-1}$ biomass) to 160 °C (106 mg $g^{-1}$ biomass). However, at 180 °C, the average xylose yield was approximately 28 mg $g^{-1}$ biomass lower than at 160 °C, with an average of 80 mg $g^{-1}$ biomass. This finding suggests a substantial impact of xylose degradation to furfural formation.

**Table 3. Arrhenius Parameters of Xylan and Glucan Hydrolysis for Miscanthus[a]**

| product | rate constant | $k_{i,\mathrm{ref}}$ [$\mathrm{min}^{-1}$] | $E_{i,\mathrm{A}}$ [kJ $\mathrm{mol}^{-1}$] |
|---|---|---|---|
| xylose | $k_{\mathrm{fx}}$ | $2.0960 \times 10^{-1}$ | 77.14 |
| | $k_{\mathrm{sx}}$ | $1.2109 \times 10^{-3}$ | 27.78 |
| glucose | $k_{\mathrm{fg}}$ | $2.1339 \times 10^{-2}$ | 162.44 |
| | $k_{\mathrm{sg}}$ | $5.8670 \times 10^{-6}$ | 728.97 |

[a]Due to the high variability in the experimental data, the kinetic parameters show only limited reliability.

**Table 4. Determined Fractions of Fast Hydrolyzing Xylan for all Temperatures for Miscanthus**

| temperature | 140 °C | 160 °C | 180 °C |
|---|---|---|---|
| $\varphi$ | 0.173 | 0.592 | 0.471 |

While glucose degradation was not observed, xylose degradation is known to occur at the applied reaction conditions in a batch reactor.[33,35]

The initial 15 min of the experiment are dominated by the hydrolysis of the fast hydrolyzing xylan, irrespective of temperature. Following this process, the curve exhibits a flattening effect, and slow hydrolyzing xylan undergoes a significantly slower and more consistent degradation. However, furfural formation significantly overshadows this effect at 180 °C. A comparison of the parameters for temperatures of 140 and 160 °C indicates that $k_{\mathrm{sx}}$, $k_{\mathrm{fx}}$, and $\varphi$ are likely to be underestimated because there is a high parameter correlation in this section, resulting in the influence of different parameters being indistinguishable. This finding suggests that the furfural



https://doi.org/10.1021/acssuschemeng.5c05534
ACS Sustainable Chem. Eng. 2026, 14, 7099−7108

kinetics at 180 °C may in fact exceed those employed in the model. The deviation arises because $k_{degx}$ was fixed from literature rather than estimated from the present data set. At 180 °C, the inferred balance between xylose formation and loss is particularly dependent on the assumed degradation kinetics. Consequently, the activation energies derived from this method are considered unreliable.

As was observed with xylose, elevated temperatures resulted in increased glucose yields. This phenomenon is further substantiated by the consistent rise in both fitting parameters, $k_{sg}$ and $k_{fg}$. The initial minutes of the experiment at 160 and 180 °C are dominated by fast hydrolyzing starch decomposition ($k_{fg} = 2.1339 \times 10^{-2}$). Subsequent to this initial phase, a continual cellulose hydrolysis dominates the glucose yield ($k_{sg} = 5.8670 \times 10^{-6}$). Cellulose demonstrates no significant contribution to glucose yield at 140 °C. Extracted glucose exhibits low concentrations, with a maximum yield of 2.4 mg $g^{-1}$ biomass. Consequently, the modeled reaction kinetics are deemed unreliable, as the distinct glucose yields derived from starch, hemicelluloses, and cellulose prove indistinguishable in velocity from one another. Consequently, the reliability of the fitted parameters is compromised at 140 °C.

At temperatures of 160 and 180 °C, the effect of additional fast and slow-degrading shares of cellulose and hemicelluloses is not as easily traced as it is in the case of beech wood. This phenomenon can be attributed to the relatively slower rate of hydrolysis of starch, along with other fast-hydrolyzing constituents of cellulose and hemicellulose, within the sample. Consequently, the initial peak becomes less pronounced.

The resulting glucose yield is predominantly influenced by cellulose degradation. The Arrhenius fit is attributable to the unreliability of the fitting parameters at 140 °C.

Comparing the two different types of biomass, furfural formation from xylose exerts a significantly greater influence on Miscanthus than on beech wood. A comparison of the yield curves at 180 °C reveals a minor influence of furfural formation on the kinetics of beech xylose, while furfural formation exhibits a significant influence on Miscanthus xylose. This difference may be attributed to the enhanced accessibility of xylan in Miscanthus compared to beech wood. As the precision of the available data for Miscanthus at 180 °C was comparatively low, therefore it is not feasible to compare these parameters. Consequently, the formation of xylose from Miscanthus biomass must occur at an earlier stage within the reactor compared to the formation from beech wood, thereby allowing for a higher rate of conversion of xylose to furfural.

The continuous formation of sugar in the model is accompanied by a gradual breakdown of xylose into furfural. However, in the experimental results this effect is less pronounced, resulting in a deviation of the model. This effect is particularly evident at 180 °C, where the model underestimates the measured data from minute 60 onward. In the case of Miscanthus, this underestimation leads to a prediction of stronger flattening than is observed in the experimental data. This phenomenon may be attributed to the less significant role played by furfural formation in beech wood. A more robust separation of hydrolysis and degradation would require explicitly fitting degradation kinetics to experimentally acquired data, which is recommended for future work.

The fitted kinetic constants indicate that cellulose hydrolysis and extraction is only weakly temperature-dependent within the investigated range, as $k_{sg}$ remains in the same order of magnitude at 160 and 180 °C for both biomasses. This suggests that, under our conditions, cellulose conversion may be governed less by intrinsic reaction kinetics and more by factors such as mass transfer, particle accessibility, or structural limitations that are not strongly accelerated by this temperature increase.

In contrast, $k_{fg}$ is substantially lower for Miscanthus than for beech wood at both 160 and 180 °C, pointing to a significantly reduced contribution of starch-related reactions compared with cellulose. A plausible explanation is that starch in Miscanthus is less accessible, potentially due to differences in granule morphology, crystallinity, and amylose−amylopectin organization, or stronger embedding within the lignocellulosic framework. Consequently, starch conversion may remain limited even at elevated temperature, which is consistent with the significantly smaller $k_{fg}$ values observed for Miscanthus.[36,37]

## CONCLUSIONS

The flow-through biphasic OrganoCat process was utilized to facilitate a time-resolved evaluation of acid-catalyzed polysaccharide hydrolysis and extraction in beech wood (hardwood) and Miscanthus (grass) at temperatures ranging from 140 to 180 °C. Across both biomasses, hemicellulose conversion dominated the early stages. Xylose, indicative of xylan hydrolysis, exhibited a maximum peak at approximately 160 to 180 °C within 10 min. However, it shifted to approximately 20 to 25 min at 140 °C, suggesting that the onset of efficient xylan hydrolysis is delayed at lower severity levels. This delay is likely attributable to substituents and acetylation effects. Xylose extraction was found to be incomplete in both cases, which is consistent with the presence of a residual, less accessible xylan fraction associated with cellulose and protected by lignin.

At 140 °C, galacturonic acid contributed a substantial share of extracted sugars (approximately 26% for beech and approximately 10% for Miscanthus), indicating that OrganoCatFT conditions render pectin-associated domains accessible that are not readily captured by conventional compositional hydrolysis of untreated biomass. The results demonstrated that glucose yield increased with temperature and exceeded the native glucan contents, which is consistent with contributions from starch, hemicellulosic glucans, and limited cellulose hydrolysis. However, the overlap of these sources limits mechanistic resolution from glucose alone.

Kinetic fitting supported a two-fraction xylan model in beech wood, with activation energies of $E_{A,fx}$ = 105 kJ $mol^{-1}$ (fast) and $E_{A,sx}$ = 144 kJ $mol^{-1}$ (slow) and an increasing fast hydrolyzing fraction, denoted by $\varphi$, which increased from 0.208 (140 °C) to 0.634 (180 °C). This finding is consistent with a transition from readily accessible xylan to more recalcitrant, cellulose-associated xylan. In Miscanthus, xylose yield increased to 106 mg $g^{-1}$ at 160 °C but declined to 80 mg $g^{-1}$ at 180 °C, consistent with increased xylose degradation to furfural at higher severity, while parameter values at 160−180 °C carry higher uncertainty due to replicate variability.

In summary, the specific xylan architecture of biomass is found to be the key factor of the initial hydrolysis behavior. Cellulose conversion exhibits a comparatively diminished temperature sensitivity within the range of 160 to 180 °C under the investigated experimental conditions. In future modeling endeavors, it is recommended to incorporate the degradation of sugar explicitly. This will serve to reduce



https://doi.org/10.1021/acssuschemeng.5c05534
ACS Sustainable Chem. Eng. 2026, 14, 7099−7108

parameter correlation and enhance the interpretability of kinetics.

## ■ ASSOCIATED CONTENT

### Data Availability Statement

The authors confirm that all primary and Supporting Information are included in the main manuscript and the Supporting Information.

### Supporting Information

The Supporting Information is available free of charge at https://pubs.acs.org/doi/10.1021/acssuschemeng.5c05534.

Additional experimental data, and graphs, including tables with individual data points from multiple measurements and a convergence plot of beech hydrolysis at 140 °C (PDF)

## ■ AUTHOR INFORMATION


### Corresponding Authors

**Holger Klose** − *Institute for Bio and Geo Sciences, Plant Sciences Forschungszentrum Jülich GmbH, 52425 Jülich, Germany; RWTH Aachen University, 52074 Aachen, Germany; Bioeconomy Science Center (BioSC) Forschungszentrum Jülich GmbH, 52425 Jülich, Germany*; Email: h.klose@fz-juelich.de

**Philipp M. Grande** − *Institute for Bio and Geo Sciences, Plant Sciences Forschungszentrum Jülich GmbH, 52425 Jülich, Germany; Bioeconomy Science Center (BioSC) Forschungszentrum Jülich GmbH, 52425 Jülich, Germany*; orcid.org/0000-0002-2137-4920; Email: p.grande@fz-juelich.de

### Authors

**Leonie Schoofs** − *Institute for Bio and Geo Sciences, Plant Sciences Forschungszentrum Jülich GmbH, 52425 Jülich, Germany; RWTH Aachen University, 52074 Aachen, Germany; Bioeconomy Science Center (BioSC) Forschungszentrum Jülich GmbH, 52425 Jülich, Germany*

**Henry Hilker** − *Institute for Bio and Geo Sciences, Plant Sciences Forschungszentrum Jülich GmbH, 52425 Jülich, Germany; Fluid Process Engineering (AVT, FVT) RWTH Aachen University, 52074 Aachen, Germany*

**Niclas Conen** − *Institute for Bio and Geo Sciences, Plant Sciences Forschungszentrum Jülich GmbH, 52425 Jülich, Germany; Bioeconomy Science Center (BioSC) Forschungszentrum Jülich GmbH, 52425 Jülich, Germany*; orcid.org/0009-0008-6714-0127

**Andreas Jupke** − *Institute for Bio and Geo Sciences, Plant Sciences Forschungszentrum Jülich GmbH, 52425 Jülich, Germany; Fluid Process Engineering (AVT, FVT) RWTH Aachen University, 52074 Aachen, Germany*; orcid.org/0000-0001-6551-5695

Complete contact information is available at: https://pubs.acs.org/10.1021/acssuschemeng.5c05534

### Author Contributions

⊥L.S. and H.H. contributed equally.


### Notes

The authors declare no competing financial interest.

## ■ ACKNOWLEDGMENTS

The authors acknowledge the financial support of the Bioeconomy Science Center as part of the project LignoTex. The scientific activities of the Bioeconomy Science Center were financially supported by the Ministry of Innovation, Science and Research within the framework of the NRW Strategieprojekt BioSC (no. 313/323-400-002 13). The authors thank Dagmar Drobietz, Benedict Ohrem, Annika Ruers, Julia Holten and Tom Hübner for their support in sample preparation and analysis.

## ■ REFERENCES


(1) Zhou, X.; Ding, D.; You, T.; Zhang, X.; Takabe, K.; Xu, F. Synergetic Dissolution of Branched Xylan and Lignin Opens the Way for Enzymatic Hydrolysis of Poplar Cell Wall. *J. Agr. Food Chem.* **2018**, *66* (13), 3449−3456.

(2) Laukkanen, J.; Mäkimartti, O.; Hannu-Kuure, M.; Hartikainen, J. Softwood-based, High-quality Organosolv Lignin as a Sustainable Raw Material for Greener and Cost-effective Industrial Applications. *Biofuel Bioprod. Bior.* **2025**, *19* (6), 1451−1455.

(3) Mosier, N.; Wyman, C.; Dale, B.; Elander, R.; Lee, Y. Y.; Holtzapple, M.; Ladisch, M. Features of Promising Technologies for Pretreatment of Lignocellulosic Biomass. *Bioresour. Technol.* **2005**, *96* (6), 673−686.

(4) Zijlstra, D. S.; Analbers, C. A.; de Korte, J.; Wilbers, E.; Deuss, P. J. Efficient Mild Organosolv Lignin Extraction in a Flow-through Setup Yielding Lignin with High $\beta$-O-4 Content. *Polymers* **2019**, *11* (12), 1913−1917.

(5) Rao, J.; Lv, Z.; Chen, G.; Peng, F. Hemicellulose: Structure, Chemical Modification, and Application. *Prog. Polym. Sci.* **2023**, *140*, 101675.

(6) Ragauskas, A. J.; Williams, C. K.; Davison, B. H.; Britovsek, G.; Cairney, J.; Eckert, C. A.; Frederick, W. J.; Hallett, J. P.; Leak, D. J.; Liotta, C. L.; Mielenz, J. R.; Murphy, R.; Templer, R.; Tschaplinski, T. The Path Forward for Biofuels and Biomaterials. *Science* **2006**, *311* (5760), 484−489.

(7) Smit, A. T.; Hoek, M.; Bonouvrie, P. A.; van Zomeren, A.; Riddell, L. A.; Bruijnincx, P. C. A. Semicontinuous Aqueous Acetone Organosolv Fractionation of Lignocellulosic Biomass: Improved Biorefinery Processing and Output. *ACS Sustain. Chem. Eng.* **2024**, *12* (11), 4731−4742.

(8) Timell, T. E. Recent Progress in the Chemistry of Wood Hemicelluloses. *Wood Sci. Technol.* **1967**, *1* (1), 45−70.

(9) Simmons, T. J.; Mortimer, J. C.; Bernardinelli, O. D.; Pöppler, A. C.; Brown, S. P.; DeAzevedo, E. R.; Dupree, R.; Dupree, P. Folding of Xylan onto Cellulose Fibrils in Plant Cell Walls Revealed by Solid-State NMR. *Nat. Commun.* **2016**, *7*, 1−9.

(10) Schoofs, L.; Weidener, D.; Leitner, W.; Klose, H.; Grande, P. M. Lignocellulose Treatment Using a Flow-Through Variant of OrganoCat Process. *ChemSusChem* **2025**, *18* (3), No. e202401063.

(11) Damm, T.; Pattathil, S.; Günl, M.; Jablonowski, N. D.; O'Neill, M.; Grün, K. S.; Grande, P. M.; Leitner, W.; Schurr, U.; Usadel, B.; Klose, H. Insights into Cell Wall Structure of Sida Hermaphrodita and Its Influence on Recalcitrance. *Carbohyd. Polym.* **2017**, *168*, 94−102.

(12) Foster, C. E.; Martin, T. M.; Pauly, M. Comprehensive Compositional Analysis of Plant Cell Walls (Lignocellulosic Biomass) Part I: Lignin. *J. Vis. Exp.* **2010**, No. 37, 5−8.

(13) Foster, C. E.; Martin, T. M.; Pauly, M. Comprehensive Compositional Analysis of Plant Cell Walls (Lignocellulosic Biomass) Part II: Carbohydrates. *J. Vis. Exp.* **2010**, No. 37, 10−13.

(14) Zhang, R.; Lu, X.; Sun, Y.; Wang, X.; Zhang, S. Modeling and Optimization of Dilute Nitric Acid Hydrolysis on Corn Stover. *J. Chem. Technol. Biot.* **2011**, *86* (2), 306−314.

(15) Kobayashi, T.; Sakai, Y. Hydrolysis Rate of Pentosan of Hardwood in Dilute Sulfuric Acid. *B. Agr. Chem. Soc. Japan* **1956**, *20* (1), 1−7.

(16) Toor, S. S.; Rosendahl, L.; Rudolf, A. Hydrothermal Liquefaction of Biomass: A Review of Subcritical Water Technologies. *Energy* **2011**, *36* (5), 2328−2342.
(17) Wang, B.; Chen, K.; Zhang, P.; Long, L.; Ding, S. Comparison of the Biochemical Properties and Roles in the Xyloglucan-Rich Biomass Degradation of a GH74 Xyloglucanase and Its CBM-Deleted Variant from Thielavia Terrestris. *Int. J. Mol. Sci.* **2022**, *23* (9), 5276.
(18) Lu, X.; Junghans, P.; Weckesser, S.; Wärnå, J.; Hilpmann, G.; Lange, R.; Trajano, H.; Eränen, K.; Estel, L.; Leveneur, S.; Grénman, H. One Flow through Hydrolysis and Hydrogenation of Semi-Industrial Xylan from Birch (Betula Pendula) in a Continuous Reactor Kinetics and Modelling. *Chem. Eng. Process.* **2021**, *169* (September), 108614.
(19) Na, B.-I.; Lee, J.-W. Kinetic Study on the Dilute Acid Catalyzed Hydrolysis of Waste Mushroom Medium. *J. Ind. Eng. Chem.* **2015**, *25*, 176−179.
(20) Hongsiri, W.; Danon, B.; de Jong, W. The Effects of Combined Catalysis of Oxalic Acid and Seawater on the Kinetics of Xylose and Arabinose Dehydration to Furfural. *Int. J. Energy Environ. Eng.* **2015**, *6* (1), 21−30.
(21) Arufe, S.; Hellouin de Menibus, A.; Leblanc, N.; Lenormand, H. Physico-Chemical Characterisation of Plant Particles with Potential to Produce Biobased Building Materials. *Ind. Crop. Prod.* **2021**, *171* (August), 113901.
(22) Scholz, G.; Zauer, M.; Van den Bulcke, J.; Van Loo, D.; Pfriem, A.; Van Acker, J.; Militz, H. Investigation on Wax-Impregnated Wood. Part 2: Study of Void Spaces Filled with Air by He Pycnometry, Hg Intrusion Porosimetry, and 3D X-Ray Imaging. *Holzforschung* **2010**, *64* (5), 587−593.
(23) Cheng, K.; Sorek, H.; Zimmermann, H.; Wemmer, D. E.; Pauly, M. Solution-State 2D NMR Spectroscopy of Plant Cell Walls Enabled by a Dimethylsulfoxide-D6/1-Ethyl-3-Methylimidazolium Acetate Solvent. *Anal. Chem.* **2013**, *85* (6), 3213−3221.
(24) Johnson, A. M.; Kim, H.; Ralph, J.; Mansfield, S. D. Natural Acetylation Impacts Carbohydrate Recovery during Deconstruction of Populus Trichocarpa Wood. *Biotechnol. Biofuels* **2017**, *10* (1), 1−12.
(25) Vogel, J. Unique Aspects of the Grass Cell Wall. *Curr. Opin. Plant Biol.* **2008**, *11* (3), 301−307.
(26) Kirui, A.; Zhao, W.; Deligey, F.; Yang, H.; Kang, X.; Mentink-Vigier, F.; Wang, T. Carbohydrate-Aromatic Interface and Molecular Architecture of Lignocellulose. *Nat. Commun.* **2022**, *13* (1), 1−12.
(27) Gao, Y.; Lipton, A. S.; Wittmer, Y.; Murray, D. T.; Mortimer, J. C. A Grass-Specific Cellulose-Xylan Interaction Dominates in Sorghum Secondary Cell Walls. *Nat. Commun.* **2020**, *11* (1), 1−10.
(28) Kang, X.; Kirui, A.; Dickwella Widanage, M. C.; Mentink-Vigier, F.; Cosgrove, D. J.; Wang, T. Lignin-Polysaccharide Interactions in Plant Secondary Cell Walls Revealed by Solid-State NMR. *Nat. Commun.* **2019**, *10* (1), 347.
(29) Heinonen, E.; Sivan, P.; Jiménez-Quero, A.; Lindström, M. E.; Wohlert, J.; Henriksson, G.; Vilaplana, F. Pattern of Substitution Affects the Extractability and Enzymatic Deconstruction of Xylan from Eucalyptus Wood. *Carbohyd. Polym.* **2025**, *353* (January), 123246.
(30) Del Río, J. C.; Marques, G.; Rencoret, J.; Martínez, A. T.; Gutiérrez, A. Occurrence of Naturally Acetylated Lignin Units. *J. Agr. Food Chem.* **2007**, *55* (14), 5461−5468.
(31) Yuan, Q.; Liu, S.; Ma, M.-G.; Ji, X.-X.; Choi, S.-E.; Si, C. The Kinetics Studies on Hydrolysis of Hemicellulose. *Front. Chem.* **2021**, *9* (November), 781291.
(32) Maloney, M. T.; Chapman, T. W.; Baker, A. J. Dilute Acid Hydrolysis of Paper Birch: Kinetics Studies of Xylan and Acetyl-group Hydrolysis. *Biotechnol. Bioeng.* **1985**, *27* (3), 355−361.
(33) Weidener, D.; Leitner, W.; Domínguez de María, P.; Klose, H.; Grande, P. M. Lignocellulose Fractionation Using Recyclable Phosphoric Acid: Lignin, Cellulose, and Furfural Production. *ChemSusChem* **2021**, *14*, 909−916.
(34) Gurgel, L. V. A.; Marabezi, K.; Zanbom, M. D.; Curvelo, A. A. D. S. Dilute Acid Hydrolysis of Sugar Cane Bagasse at High Temperatures: A Kinetic Study of Cellulose Saccharification and Glucose Decomposition. Part I: Sulfuric Acid as the Catalyst. *Ind. Eng. Chem. Res.* **2012**, *51* (3), 1173−1185.
(35) Weidener, D.; Klose, H.; Leitner, W.; Schurr, U.; Usadel, B.; Domínguez de María, P.; Grande, P. M. One-Step Lignocellulose Fractionation by Using 2,5-Furandicarboxylic Acid as a Biogenic and Recyclable Catalyst. *ChemSusChem* **2018**, *11* (13), 2051−2056.
(36) Blazek, J.; Gilbert, E. P. Effect of Enzymatic Hydrolysis on Native Starch Granule Structure. *Biomacromolecules* **2010**, *11* (12), 3275−3289.
(37) Chen, X.; Zhu, L.; Zhang, H.; Wu, G.; Cheng, L.; Zhang, Y. A Review of Endogenous Non-Starch Components in Cereal Matrix: Spatial Distribution and Mechanisms for Inhibiting Starch Digestion. *Crc. Cr. Rev. Food Sci.* **2025**, *65* (19), 3686−3701.




https://doi.org/10.1021/acssuschemeng.5c05534
ACS Sustainable Chem. Eng. 2026, 14, 7099−7108